agriculture

MDPI

Article

Dynamically Updated Irrigation Canal Scheduling Rules Based on Risk Hedging

Ming Yan [1], Fengyan Wu [2], Luli Chen [3], Yong Liu [4], Xiang Zeng [5] and Tiesong Hu [1,*]

[1] State Key Laboratory of Water Resources Engineering and Management, Wuhan University, Wuhan 430072, China; yanming@whu.edu.cn
[2] Hubei International Irrigation and Drainage Research and Training Center, Hubei Water Resources Research Institute, Wuhan 430070, China
[3] Department of Hydraulic Engineering, Hubei Water Resources Technical College, Wuhan 430070, China
[4] National Engineering Research Center of Eco-Environment in the Yangtze River Economic Belt, China Three Gorges Corporation, Wuhan 430010, China
[5] School of Resource and Environmental Sciences, Wuhan University, Wuhan 430079, China
* Correspondence: tshu@whu.edu.cn

Abstract

Dynamic canal-system scheduling faces the fundamental challenge of determining the optimal reduction in the current period's water allocation to reserve sufficient water for remaining periods, thereby hedging against potentially greater future water shortages. Although forecast information has been widely incorporated to address this hedging problem, its effectiveness is heavily dependent on forecast accuracy. Integrating abundant historical canal scheduling data with forecast information provides a promising pathway to improve scheduling performance, yet relevant studies remain limited. This study introduces the concept of Target Residual Lump-Sum Water Quota (*TRLSWQ*) for each time interval and develops a novel "Bi-level, Two-stage" (BT) model for dynamically updated canal-system scheduling that jointly leverages *TRLSWQ* and forecast information. The model defines clear canal scheduling rules and effectively adapts to the hierarchical structure in canal system scheduling. The model is applied to the summer–autumn irrigation scheduling of the Yongji main canal and six associated sub-canals in the Hetao Irrigation Area, Inner Mongolia, China. The results indicate that compared with the conventional model, the BT model reduces the total water shortage index of sub-canals from 40.81 to 31.44 (a decrease of 22.9%) and increases the utilization rate of the water quota from 89.3% to 92.9% (an increase of 3.9%). Furthermore, this study clarifies the mechanism of canal scheduling deviations caused by forecast errors: early-stage rainfall under-forecasting induces excessive early-stage allocation, leaving no water for later periods, whereas early-stage over-forecasting leads to withheld early allocation and unused residual lump-sum quota in later stages. The BT model effectively balances shortage risks between current and future periods and offers a practical and robust strategy for improving dynamic canal scheduling in irrigation districts.

Keywords: irrigation canal system; dynamically updated canal scheduling; "Bi-level, Two-stage" (BT) model; risk hedging; hedging rules

Academic Editor: Jeff Strock

Received: 17 November 2025
Revised: 3 December 2025
Accepted: 4 December 2025
Published: 5 December 2025

Citation: Yan, M.; Wu, F.; Chen, L.; Liu, Y.; Zeng, X.; Hu, T. Dynamically Updated Irrigation Canal Scheduling Rules Based on Risk Hedging. *Agriculture* **2025**, *15*, 2527. https://doi.org/10.3390/agriculture15242527

1. Introduction

Water scarcity is one of the most severe challenges facing the world in the 21st century. Over 70% of extracted freshwater resources are consumed by global irrigated agriculture [1], with canal water delivery efficiency in numerous traditional irrigation areas still falling below 60% [2]. Therefore, improving irrigation water-use efficiency is of great urgency, and its enormous potential in alleviating water resource scarcity remains largely untapped [3,4]. In this context, optimal canal system scheduling technology, as a key breakthrough in agricultural water resource management, has attracted extensive attention globally.

The canal system scheduling aims to optimize water distribution among multi-level canal systems based on real-time soil moisture conditions, farmers' declared use plans, and forecasted inflow at canal heads, thereby generating coordinated operational schedules for both main and subsidiary canals. Through the simulation of canal control and crop growth processes, the scheduling objective is to achieve the optimal spatiotemporal distribution of agricultural water resources and ensure smooth canal operation, while meeting crop water requirements and adhering to constraints related to canal safety and ecological conditions [5,6]. Proper canal scheduling minimizes deviations between the planned water consumption process and the water allocation process, thereby reducing the risk of water scarcity and conveyance losses. Conversely, an unsuitable canal scheduling may cause the water delivery process to overlap with rainfall events, force primary canals to operate at high load for extended periods during peak-demand stages, or lead to prolonged semi-capacity operation of the canal system [7,8]. Such circumstances can lead to crop losses due to waterlogging, damage to canal system structures, and increased seepage losses during water conveyance.

The canal scheduling system is a complex system involving multiple stakeholders, multiple levels, and multiple dimensions, including government bodies, farmers, and administrators of main, branch, lateral, and field canals. Since Suryavanshi and Reddy [9] pioneered the 0–1 programming method to study the optimal grouping of lower-level canals, scholars have conducted extensive research on canal system scheduling optimization, transitioning from traditional empirical methods to more scientific and precise optimization strategies [10]. The development of irrigation canal scheduling can generally be categorized into three phases: the initial experience-based phase relying on managers' personal expertise [11], the simulation–optimization phase integrating optimization models with canal system hydrodynamic simulation models, and the current intelligent and informatized phase using new technologies such as decision-making based on big data and artificial intelligence. Over the past four decades, the scope of research on canal scheduling has expanded. It has evolved from solely studying the optimal grouping problem of terminal canal systems under the scenario of "fixed flow rate and variable duration" [9] to the grouping problem under "variable flow rate and variable duration" [12]. Subsequently, it has gradually extended to researching issues such as the schedule of the entire canal system, including how to group terminal canals and how to implement continuous water conveyance in main canals, the coordination between canal scheduling and canal gate control [10], and the collaborative optimization between canal system scheduling and water resource allocation in irrigation districts [13]. The canal scheduling models have developed from the initial single-agent single-objective or multi-objective optimization models [11,14,15] to the present multi-agent, multi-level [6], and multi-objective models [5,16]. The algorithms used to solve these models have progressed from initial mathematical programming algorithms (e.g., the simplex method) to modern intelligent optimization algorithms such as the simulated annealing algorithm [17], genetic algorithm [18,19], ant colony algorithm [20], backtracking search algorithm [21], and particle swarm optimization algorithm [22]. Additionally, modern technologies such as machine learning have

been applied to canal scheduling [23]. The above-mentioned studies have established a rich foundation for optimizing scheduling in canal systems.

Despite these advancements, a primary challenge in current research on optimal canal system scheduling is that the resulting canal schedules often have limited practical applicability in enhancing operational efficiency. These schedules typically involve extended time horizons, such as schedules for annual, irrigation seasons, crop growth stages, or individual irrigation events. These canal schedules are generally static and are developed based on historical canal schedules and fixed crop growth calendars. In the context of increasing hydrological variability due to climate change and rapid shifts in crop planting structures, such static schedules struggle to respond effectively to unforeseen meteorological events, such as short-term rainfall, heatwaves, or droughts. Therefore, leveraging the latest soil moisture monitoring data and short-term hydrometeorological forecasts to formulate canal operation schedules for single irrigation events in canal systems and update these schedules dynamically in real time to achieve precise and efficient spatial–temporal allocation of the total irrigation water in canal systems constitutes an effective approach to improving the scheduling efficiency of canal systems. However, to the best of the authors' knowledge, there are currently very few studies reporting models or algorithms for dynamically updated irrigation canal scheduling [10,24]. Although in practical irrigation district management, rolling canal water distribution planning with a 5-day cycle has been issued [25,26], and a substantial body of research has reported methods for formulating rolling or real-time irrigation schedules [27–30] as well as reservoir operation schemes [31,32].

Under the constraint of a fixed initial lump-sum water quota (*ILSWQ*) for the entire crop growth stage, the dynamically updated canal scheduling requires decisions regarding the water allocation volume at each canal system's intake for the current period. Specifically, it must determine whether to fully meet the water intake demand or only partially fulfill it, in order to mitigate the potential risk of greater water shortages in subsequent periods. Traditional methods for dynamically updating irrigation plans balance water allocation volumes between the current and future periods by assuming that hydrometeorological forecasts for the remaining period are entirely accurate. If this assumption holds, such a balancing strategy may be considered optimal. However, this strategy presents two key limitations: first, accurate hydrometeorological forecasts for the crop growth period are inherently difficult to achieve [30]; second, relying solely on forecast data while neglecting long-term historical canal scheduling information is inadequate. The risk hedging strategy, as proposed by the two-stage model, offers a novel perspective and valuable insight for addressing these limitations. This approach has been widely applied in both theoretical research and practical applications in reservoir operation. As early as more than sixty years ago, Maass et al. [33] first introduced the risk hedging strategy into reservoir operation, aiming to offset the risk of potentially unacceptable severe water shortages in the future through tolerable minor water shortages during a series of current periods. Draper and Lund [34], along with You and Cai [35], have provided comprehensive reviews on the evolution of hedging methods in reservoir operations. Zeng et al. [36] extended this approach to parallel reservoir systems, developing a two-stage joint operation model and proposing new joint operation rules with analytical expressions. In canal system scheduling decision-making, the *ILSWQ* can be regarded as stored in a virtual reservoir, and the water allocation process for each canal in each period can be determined by applying similar hedging rules. By incorporating information from historical canal scheduling processes and analyzing the temporal variation in residual lump-sum water quota (*RLSWQ*) across different years, the canal scheduling hedging rules can reasonably control the timeline of water volume release in the virtual reservoir, avoid artificial water shortages or waste, and help enhance the stability of canal scheduling processes.

However, to date, there is no reported research on the application of risk hedging principles to the dynamically updated canal scheduling process.

This study aims to: (1) explore and propose a dynamically updated canal scheduling framework that reduces current-period water allocation to increase remaining-period allocation, hedging against future water shortage risks; (2) study the balance strategy between current and remaining-period water shortage risks; (3) establish a new dynamically updated canal scheduling model integrating hydrometeorological forecast information and long-term historical canal scheduling data of irrigation districts; and (4) analyze the model performance and the mechanism of canal scheduling deviations caused by forecast errors.

The remainder of this paper is organized as follows: Section 2 establishes a "Bi-level, Two-stage" model for the dynamically updated canal scheduling, which comprises a canal scheduling rule optimization model and a crop water demand forecast model. Section 3 conducts a case study focusing on the canal system scheduling in the crop growth stage in the Yongji Irrigation District of the Hetao Irrigation Area, Inner Mongolia, China, and demonstrates the performance of different canal scheduling models. Section 4 analyzes and discusses the canal scheduling results and strategies in the case study, as well as the limitations of the BT model. Section 5 presents the conclusions and research prospects of this study.

2. Materials and Methods

This study focuses on a two-level canal scheduling system encompassing water sources, a main canal, and sub-canals (as shown in Figure 1).

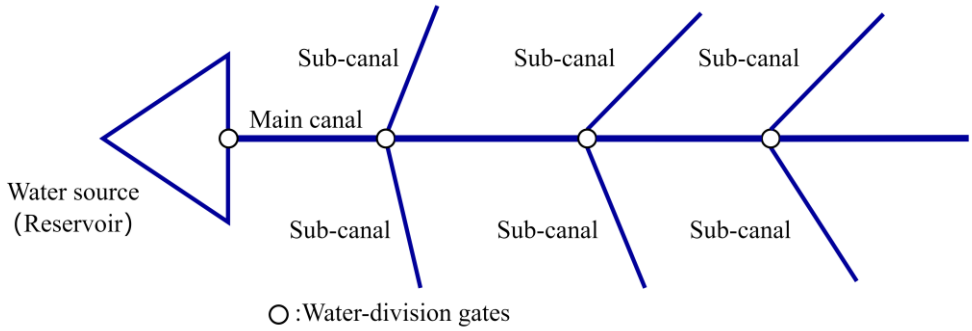

Figure 1. Conceptual diagram of a single water source irrigation canal system.

Different from the black-box operation of conventional dynamically updated canal scheduling practice based solely on forecast information, this study assumes that dynamically updated canal scheduling determines the water allocation volumes for the main canals and sub-canals illustrated in Figure 1 by integrating the latest hydrometeorological forecast information and historical canal schedule data in accordance with specific canal scheduling rules. The canal scheduling rules include two key water volume parameters: first, the *TRLSWQ* that the water source should retain in each period to meet crop water demand; second, the threshold water volume (*TWV*) triggering water supply reduction in each current period to mitigate the risk of more severe water shortages in subsequent periods. These two parameters complement and are interrelated with each other: a higher *TRLSWQ* allows for a lower *TWV*. Canal scheduling decisions are made in accordance with predefined rules at any given period of any year. The entire decision-making process for the distribution period is carried out in multiple steps. At the beginning of each period, the *TRLSWQ* for the current period, the forecast maximum water supply, and the water demand are input, and the water allocation volume of each outlet of the canal system for

that period is determined based on the established rules. After the implementation of the canal schedule for one period is completed, the latest forecast information is updated for the start of the next period, and the canal schedule decision for the next period is continued. This process rolls forward sequentially from one period to the next until the canal schedules for all periods are finalized.

The following section provides a detailed introduction to the "Bi-level, Two-stage" dynamically updated canal scheduling model and presents the method for determining its canal scheduling rules. To compare the performance of different canal scheduling strategies, this study also introduces the conventional dynamically updated canal scheduling model based on forecast information (abbreviated as the CC model) and the optimal static canal scheduling model (abbreviated as the OC model), which assumes the hydrometeorological forecasts are entirely accurate. All models were written and executed in Fortran, using the Intel Fortran Compiler (version 2021.3.0) within the Microsoft Visual Studio Community 2019 software platform.

The definitions of all variables and parameters in the models are listed in Table 1.

Table 1. Nomenclature.

Variables/Parameters		Definition	Unit
Parameters and variables required for model optimization	$R_{y,t,k}$	the outlet water volume of the *k*-th sub-canal in the *t*-th period of the *y*-th year	m^3
	$D_{y,t,k}$	the water demand of the *k*-th sub-canal in the *t*-th period of the *y*-th year	m^3
	$DF_{y,ta,tb,k}$	the forecast value of the water demand of the *k*-th sub-canal in *tb*-th period of *y*-th year from the beginning of the *ta*-th period of *y*-th year	m^3
	$TRLSWQ_t$	the target residual lump-sum water quota at the beginning of the *t*-th period	m^3
	$ILSWQ_y$	the initial lump-sum water quota of the *y*-th year's crop growth stage	m^3
	$TWV_{t,k}$	the threshold water volume of the *t*-th period of the *k*-th sub-canal	m^3
	$OBJU$	the objective function value of the upper-level model of the BT model	
	$OBJLM_k, OBJL_{y,t,k}$	the objective function value of the *k*-th sub-canal of the lower-level model of the BT model, the canal schedule efficiency loss of the BT model at the *t*-th period of the *y*-th year of the *k*-th sub-canal	
	$DevD, DevT$	the deviation between water allocation and demand of the current period, the deviation between the residual lump-sum water quota and the target residual lump-sum water quota at the end of the current period	
	$RLSWQ_{y,t}$	the residual lump-sum water quota of the *t*-th period in the *y*-th year	m^3
	$MWS_{y,t}$	the maximum water supply of the *t*-th period in the *y*-th year	m^3
	$MRG_{y,t}$	the inlet water volume of the main canal in the *t*-th period of the *y*-th year	m^3
	$MRGD_{y,t}$	the on-demand inlet water volume of the main canal in the *t*-th period of the *y*-th year	m^3
	$R'_{y,t,k}$	the limited outlet water volume of the *k*-th sub-canal in the *t*-th period of the *y*-th year, while the maximum water supply can meet the water demand	m^3
	$R''_{y,t,k}$	the limited outlet water volume of the *k*-th sub-canal in the *t*-th period of the *y*-th year, while the maximum water supply or residual lump-sum water quota cannot meet the water demand	m^3
	$TWL_{y,t}$	the total water loss of the canal system in the *t*-th period of the *y*-th year	m^3
	α, β	empirical parameters for water loss calculation	

	ls_k	length of the *k*-th sub-canal	km
	lm_j	length of the *j*-th part of the main canal (where *j* = 1 denotes the initial section of the main canal, and *j* = *J* denotes the terminal section of the main canal)	km
	$MRN_{y,t,j}$	outlet water volume of the *j*-th section of the main canal in the *t*-th period of the *y*-th year	m^3
	k_{js}, k_{je}	the starting and ending numbers of the sub-canals directly connected to the *j*-th section of the main canal	
	Δt	the duration of a period	d
	$MR_{\max}$	the designed discharge of the main canal	m^3/s
	$R_{\max,k}$	the designed discharge of the *k*-th sub-canal	m^3/s
	$OBJC_{y,ta}$	the objective function value of the CC model at the beginning of the *ta*-th period of the *y*-th year	
	$OBJO_y$	the objective function value of the OC model	
Parameters required for water demand calculation	$ET_{y,t,m}$	the evapotranspiration of the *m*-th crop in the *t*-th period of the *y*-th year	mm
	$K_{c,m}$	the crop coefficient of the *m*-th crop	
	K_s	soil moisture correction coefficient, its value is set to 1	
	$ET_{0,y,t}$	reference evapotranspiration in the *t*-th period of the *y*-th year	mm
	$SW_{y,t,k,m}$	the soil moisture content of the tillage layer of the *m*-th crop in the *t*-th period of the *y*-th year in the field irrigated by the *k*-th sub-canal	mm
	$SWR_{y,t,k,m}$	the change in soil moisture content caused by the variation in the depth of the tillage layer of the *m*-th crop in the *t*-th period of the *y*-th year in the field irrigated by the *k*-th sub-canal	mm
	$SWO_{y,t,k,m}$	the soil moisture content of the tillage layer of the *m*-th crop in *t*-th period of *y*-th year in the field irrigated by the *k*-th sub-canal, assuming no irrigation is conducted during the (*t* − 1)-th period	mm
	$PF_{y,t}$	the forecast effective precipitation in the *t*-th period of the *y*-th year	mm
	$P_{y,t}$	the observed effective precipitation in the *t*-th period of the *y*-th year	mm
	$PE_{y,t}$	the forecast error of effective precipitation in the *t*-th period of the *y*-th year	mm
	η	the ratio of the standard deviation of the normal distribution of the forecast error of effective precipitation that the error follows to the observed value	
	$U_{y,t,k,m}$	groundwater recharge to the tillage layer of the *m*-th crop in *t*-th period of *y*-th year in the field irrigated by the *k*-th sub-canal	mm
	$I_{y,t,k,m}$	irrigation water volume per unit area of the *m*-th crop in the *t*-th period of the *y*-th year in the field irrigated by the *k*-th sub-canal	mm
	$SWU_{t,m}, SWL_{t,m}$	the upper and lower limits of the suitable soil moisture content of the tillage layer of the *m*-th crop in the *t*-th period	mm
	$A_{k,m}$	planting area of the *m*-th crop in the field irrigated by the *k*-th sub-canal	m^2
Subscripts and their maximum value	y, Y	annual number, total number of years in the calculation series	
	t, T	period number within a year, total number of periods in a year	
	m, M	crop number, total number of crops	
	k, K	sub-canal number, total number of sub-canals	
	j, J	section number of the main canal, total section number of the main canal	

Performance evaluation indicators	$SWSI_y$	sum of water shortage index of all sub-canals in the y-th year	
	$TWLR_y$	canal system water loss rate in the y-th year	%
	$URILSWQ_y$	utilization rate of the initial lump-sum water quota in the y-th year	%

2.1. The "Bi-Level, Two-Stage" Dynamically Updated Canal Scheduling Model

2.1.1. Canal Scheduling Rule Optimization Model

A single canal scheduling process is divided into two phases in the BT model: the current period and the remaining period (excluding the current period). The optimizations of *TRLSWQ* and *TWV* are, respectively, designated as the upper and lower levels of the Bi-level structure for separate optimization. The optimization of *TWV* involves solving a parametric programming problem with *TRLSWQ* as the parameter, where the upper-level specifies *TRLSWQ*. The purpose of adopting the Bi-level optimization in the BT model is to reflect the hierarchical governance of canal system scheduling: the upper-level agent (e.g., the main canal administrator) aims to regulate the use of the *RLSWQ* over the entire irrigation district and time horizon to maximize system-wide benefit, whereas each lower-level agent (e.g., the sub-canal management agency) seeks, subject to the *TRLSWQ* given by the upper-level, to optimize sub-canal scheduling performance within its own control area.

The upper-level takes the *TRLSWQ* as the decision variable and transmits a set of obtained values to the lower-level each time during the optimization process. The lower-level, when the *TRLSWQ* is given by the upper-level each time, takes the minimum two-stage canal schedule efficiency loss as the objective function, takes the *TWV* as the decision variable, calculates the corresponding canal schedule process for each period, and feeds it back to the upper-level to derive the value of the upper-level objective function. By solving the Bi-level programming, the *TRLSWQ* and *TWV* of the model are finally determined. The optimization process of the model is illustrated in Figure 2.

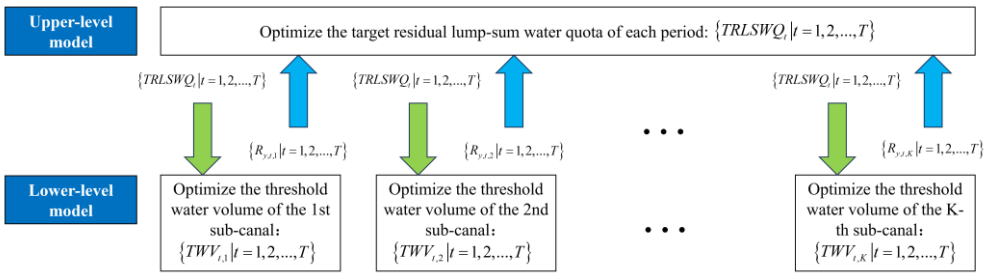

Figure 2. Schematic diagram of the "Bi-level, Two-stage" dynamically updated canal scheduling (BT) model's optimization process. Note: *TRLSWQ* means the target residual lump-sum water quota, *TWV* means the threshold water volume, and *R* means the outlet water volume.

The mathematical formulation of the Bi-level model for the BT model's optimization process is as follows.

Upper-level model:

The upper-level model takes the minimization of the multi-year sum of water shortage index of all sub-canals (*SWSI*) as the objective function, takes the $\{TRLSWQ_t|t = 1,2,\ldots,T\}$ as the decision variable, and takes the variation range of *TRLSWQ* and the period-by-period decrease in its value as the constraints.

Objective function:

$$\min OBJU = \frac{100}{Y \cdot T} \sum_{y=1}^{Y} \sum_{t=1}^{T} \sum_{\substack{k=1 \\ D_{y,t,k}>0}}^{K} \left(\frac{R_{y,t,k} - D_{y,t,k}}{D_{y,t,k}} \right)^2 \quad (1)$$

Subject to:

TRLSWQ is non-negative and not greater than the maximum value of the *ILSWQ* in the calibration period.

$$0 \le TRLSWQ_t \le \max_{y=1,2,\ldots,Y} ILSWQ_y \quad (2)$$

TRLSWQ in the subsequent period is not greater than the corresponding value in the preceding period.

$$TRLSWQ_{t+1} \le TRLSWQ_t \quad (t = 1,2,\ldots,T-1) \quad (3)$$

Lower-level model:

The lower-level model takes the minimization of the multi-year summation of canal schedule efficiency loss as the objective function, takes the $\{TWV_{t,k} | t = 1,2,\ldots,T; k = 1,2,\ldots,K\}$ as the decision variable, and takes the variation range of *TWV*, the canal schedule rules, and the water balance as the constraints.

Objective function:

$$\min OBJLM_k = \sum_{y=1}^{Y} \sum_{t=1}^{T} OBJL_{y,t,k} \quad (4)$$

The canal schedule efficiency loss of each period is equal to the sum of the deviation of water allocation (*R*) and demand (*D*) of the current period, and the deviation of the residual lump-sum water quota (*RLSWQ*) and the *TRLSWQ* at the end of the current period.

$$OBJL_{y,t,k} = DevD + DevT \quad (5)$$

$$DevD = \begin{cases} \left(\frac{R_{y,t,k} - D_{y,t,k}}{D_{y,t,k}} \right)^2 & , \quad D_{y,t,k} > 0 \\ 0 & , \quad D_{y,t,k} = 0 \end{cases} \quad (6)$$

$$DevT = \begin{cases} \left(\frac{RLSWQ_{t+1} - TRLSWQ_{t+1}}{TRLSWQ_{t+1}} \right)^2 & , \quad TRLSWQ_{t+1} > 0 \wedge t < T \\ 0 & , \quad TRLSWQ_{t+1} = 0 \vee t = T \end{cases} \quad (7)$$

Subject to:

When the current period is the *t*-th period of the *y*-th year, the outlet water volume of the *k*-th sub-canal in the period shall be determined based on the relative magnitude of the maximum water supply (*MWS*), the residual lump-sum water quota (*RLSWQ*), the on-demand inlet water volume of the main canal (*MRGD*), and *TWV*. The specific rules are as follows:

(1) If the *MWS* is not lower than the *MRGD*, and the *RLSWQ* is not lower than the *TWV*, then allocate the water of each sub-canal on demand.

(2) If the *MWS* is not lower than the *MRGD*, and the *RLSWQ* is higher than the inlet water volume of the main canal after being restricted in accordance with the rules ($MRG_{y,t}|_{R_{y,t,k}=R'_{y,t,k}}$) and lower than the *TWV*, then restrict the water volume based on the hedging factors under this scenario, which are equal to the ratios of *RLSWQ* to each *TWV*.

(3) If the *MWS* is lower than the *MRGD* or the *RLSWQ* is lower than the inlet water volume of the main canal after being restricted in accordance with the rules

($MRG_{y,t}\big|_{R_{y,t,k}=R'_{y,t,k}}$), then restrict the water volume based on the hedging factors under this scenario: calculate the ratio of the remaining water volume (after deducting losses (*WL*) from the smaller value of *RLSWQ* and *MWS*) to the sum of the water demands of all sub-canals in this period ($\sum_{k=1}^{K} D_{y,t,k}$); these ratios are the hedging factors in this scenario.

$$R_{y,t,k}=\begin{cases} D_{y,t,k} & , \begin{cases} MWS_{y,t}\geq MRGD_{y,t} \\ RLSWQ_{y,t}\geq TWV_{t,k} \end{cases} \\ R'_{y,t,k} & , \begin{cases} MWS_{y,t}\geq MRGD_{y,t} \\ MRG_{y,t}\big|_{R_{y,t,k}=R'_{y,t,k}}\leq RLSWQ_{y,t}<TWV_{t,k} \end{cases} \\ R''_{y,t,k} & , MWS_{y,t}<MRGD_{y,t}\vee RLSWQ_{y,t}<MRG_{y,t}\big|_{R_{y,t,k}=R'_{y,t,k}} \end{cases} \tag{8}$$

$$R'_{y,t,k}=\frac{RLSWQ_{y,t}}{TWV_{t,k}}D_{y,t,k} \tag{9}$$

$$R''_{y,t,k}=\frac{\min\left(RLSWQ_{y,t},MWS_{y,t}\right)-WL_{y,t}}{\sum_{k=1}^{K}D_{y,t,k}}D_{y,t,k} \tag{10}$$

$$MRGD_{y,t}=MRG_{y,t}\big|_{R_{y,t,k}=D_{y,t,k}} \tag{11}$$

The *TWV* is not less than the maximum value of the on-demand inlet water volume of the main canal (*MRGD*) in each period of the calibration period, and not greater than the maximum value of *ILSWQ* during the calibration period.

$$\max_{y=1,2,\ldots,Y}MRGD_{y,t}\leq TWV_{t,k}\leq\max_{y=1,2,\ldots,Y}ILSWQ_{y} \tag{12}$$

The *TWV* in the subsequent period is not greater than the corresponding value in the preceding period.

$$TWV_{t+1,k}\leq TWV_{t,k}\quad(t=1,2,\ldots,T-1) \tag{13}$$

Canal system water balance constraints:

The water volume at the inlet of each canal is equal to the sum of the water volume at the outlet and the water loss.

$$MRG_{y,t}=\sum_{k=1}^{K}R_{y,t,k}+TWL_{y,t} \tag{14}$$

$$TWL_{y,t}=\sum_{k=1}^{K}\alpha\cdot ls_{k}\cdot\left(R_{y,t,k}\right)^{\beta}+\sum_{j=1}^{J}\alpha\cdot lm_{j}\cdot\left(MRN_{y,t,j}\right)^{\beta} \tag{15}$$

$$MRN_{y,t,j}=MRN_{y,t,j+1}+\alpha\cdot lm_{j}\cdot\left(MRN_{y,t,j}\right)^{\beta}+\sum_{k=k_{js}}^{k_{je}}\left(R_{y,t,k}+\alpha\cdot ls_{k}\cdot\left(R_{y,t,k}\right)^{\beta}\right) \tag{16}$$

$$MRN_{y,t,J}=\sum_{k=k_{Js}}^{k_{Je}}\left(R_{y,t,k}+\alpha\cdot ls_{k}\cdot\left(R_{y,t,k}\right)^{\beta}\right) \tag{17}$$

Residual lump-sum water quota balance constraints:

The *RLSWQ* at the beginning of the first period is equal to the *ILSWQ* of the year.

$$RLSWQ_{y,1}=ILSWQ_{y} \tag{18}$$

The *RLSWQ* at the beginning of the current period minus the water allocation volume within the current period equals the *RLSWQ* at the beginning of the next period.

$$RLSWQ_{y,t+1} = RLSWQ_{y,t} - MRG_{y,t} \tag{19}$$

Canal flow capacity and water volume upper limit constraints:

$$MRG_{y,t} \le \min\left(MR_{\max} \cdot \Delta t \cdot 86400, MWS_{y,t}, RLSWQ_{y,t}\right) \tag{20}$$

$$R_{y,t,k} + \alpha \cdot ls_k \cdot \left(R_{y,t,k}\right)^{\beta} \le R_{\max,k} \tag{21}$$

2.1.2. Water Demand Calculation Model

The water demand in this study refers to the water demand process of crops during their growth stage. It is calculated based on the field water balance, and the water demand process of the corresponding canal is obtained by summing up the water demands of various crops. When the input meteorological data are forecast values, the water demand calculated by this model is the forecast value.

The evapotranspiration of each crop is equal to the product of the reference crop evapotranspiration, the crop coefficient, and the soil moisture correction coefficient. Among these, the reference crop evapotranspiration is calculated according to the Penman-Monteith method [37]. The values of crop coefficients are listed in Table A1.

$$ET_{y,t,m} = K_{c,m} \cdot K_s \cdot ET_{0,y,t} \tag{22}$$

Water balance in the field.

$$SW_{y,t+1,k,m} = SW_{y,t,k,m} + SWR_{y,t,k,m} + PF_{y,t} + U_{y,t,k,m} + I_{y,t,k,m} - ET_{y,t,m} \tag{23}$$

The forecast effective precipitation is generated by adding a normally distributed error to the observed effective precipitation.

$$\begin{cases} PF_{y,t} = P_{y,t} + PE_{y,t} \\ PE_{y,t} \sim N\left(0, \left(\eta P_{y,t}\right)^2\right) \end{cases} \tag{24}$$

For a specific crop, the judgment is based on the assumed field soil moisture content at the end of the current period without irrigation. If this moisture content is lower than the lower limit of the suitable soil moisture content, it is determined that irrigation should be carried out in this period. The water demand per unit area is the amount of water required to bring the field soil moisture content up to the upper limit of the suitable soil moisture content. The values of *SWU* and *SWL* are listed in Table A2.

The soil moisture content at the end of the current period, assuming no irrigation is conducted during the current period:

$$SWO_{y,t+1,k,m} = SW_{y,t,k,m} + SWR_{y,t,k,m} + PF_{y,t} + U_{y,t,k,m} - ET_{y,t,m} \tag{25}$$

The irrigation depth is calculated in accordance with the above-mentioned principles.

$$I_{y,t,k,m} = \begin{cases} 0 & , \quad SWO_{y,t+1,k,m} > SWL_{t,m} \\ SWU_{t+1,m} - SW_{y,t,k,m} - SWR_{y,t,k,m} & \\ -PF_{y,t} - U_{y,t,k,m} + ET_{y,t,m} & , \quad SWO_{y,t+1,k,m} \le SWL_{t,m} \end{cases} \tag{26}$$

The water demand of each sub-canal is equal to the sum of the products of the water demand per unit area of each crop and its planting area within the area controlled by the canal.

$$D_{y,t,k} = \sum_{m=1}^{M} \frac{I_{y,t,k,m}}{1000} \cdot A_{k,m} \tag{27}$$

2.2. Comparison Models

2.2.1. The Conventional Dynamically Updated Canal Scheduling Model

In each current period, the CC model makes decisions based on the forecast information of each period from the current period to the end of the decision-making period. When the current period is the *ta*-th period, the required water demand forecasting process (*DF*s) covers the entire periods from the *ta*-th period to the *T*-th period (the last period of the canal scheduling decision-making periods). This process is derived by inputting the meteorological forecast of the corresponding periods into the water demand calculation model specified in Section 2.1.2. The decision variables are the canal schedules for each period from the current period to the end of the decision-making period, and the objective function is to minimize the sum of water shortage indices for the sub-canals during the decision-making period. During the application process, only the canal schedule for the current period (the *ta*-th period), specifically the first period obtained through optimization, is implemented. After the canal schedule for the current period is completed, the forecast information is updated (the periods from the $(ta+1)$-th period to the *T*-th period), and the following decision-making process is initiated. The canal schedule for each subsequent period is carried out in accordance with the same procedure until the canal schedule for all periods is completed.

The mathematical form of the CC model is as follows.

In the *y*-th year, when the current period is the *ta*-th period:

Decision variable:

The outlet water volume of all sub-canals from *ta*-th period to *T*-th period in the *y*-th year: $\left\{R_{y,t,k} \middle| t = ta, ta+1, ..., T; k = 1, 2, ..., K\right\}$.

Objective function:

$$\min OBJC_{y,ta} = \frac{100}{T - ta + 1} \sum_{t=ta}^{T} \sum_{\substack{k=1 \\ DF_{y,ta,t,k} > 0}}^{K} \left(\frac{R_{y,t,k} - DF_{y,ta,t,k}}{DF_{y,ta,t,k}} \right)^2 \tag{28}$$

Subject to:

Constraints are the same as Equations (14)–(21).

2.2.2. The Optimal Static Canal Scheduling Model

On the premise that the *MWS* and *D* for all periods within the decision periods are accurate, the OC model directly takes the canal schedules for all periods within the year as the decision variable, with the objective function of minimizing the annual water shortage index. The canal scheduling results of this model are optimal in all years of the verification period and will be used as a reference for other models.

The mathematical form of the OC model is as follows.

Decision variable:

The outlet water volume of all sub-canals of all periods in the *y*-th year: $\left\{R_{y,t,k} \middle| t = 1, 2, ..., T; k = 1, 2, ..., K\right\}$.

Objective function:

$$\min OBJO_{y} = \frac{100}{T} \sum_{t=1}^{T} \sum_{\substack{k=1 \\ D_{y,t,k} > 0}}^{K} \left(\frac{R_{y,t,k} - D_{y,t,k}}{D_{y,t,k}} \right)^2 \tag{29}$$

Subject to:

Constraints are the same as Equations (14)–(21).

2.3. Study Area

This study focuses on the Yongji Irrigation District, a part of the Hetao Irrigation Area, as its study area. The Hetao Irrigation Area is a vast irrigation area situated in the Inner Mongolia Autonomous Region, China, covering an irrigated area of over 7600 km². Yongji Irrigation District is an important part of the Hetao Irrigation Area. The general location of the Yongji Irrigation District within the Hetao Irrigation Area, along with the structure of its primary canal system, is shown in Figure 3. This study generalizes the canal system of the Yongji Irrigation District into a two-level canal system. All water for the Yongji Irrigation District is sourced from the Hatao main canal. It is then distributed via the Yongji main canal to six sub-canals: Yonglan (YL), Yonggang (YG), Xile (XL), Xinhua (XH), Zhengshao (ZS), and Datuishui (DTS). The main crops grown in the Yongji Irrigation District are wheat, corn, and sunflowers. Irrigation during the growth stage begins in April and continues until September.

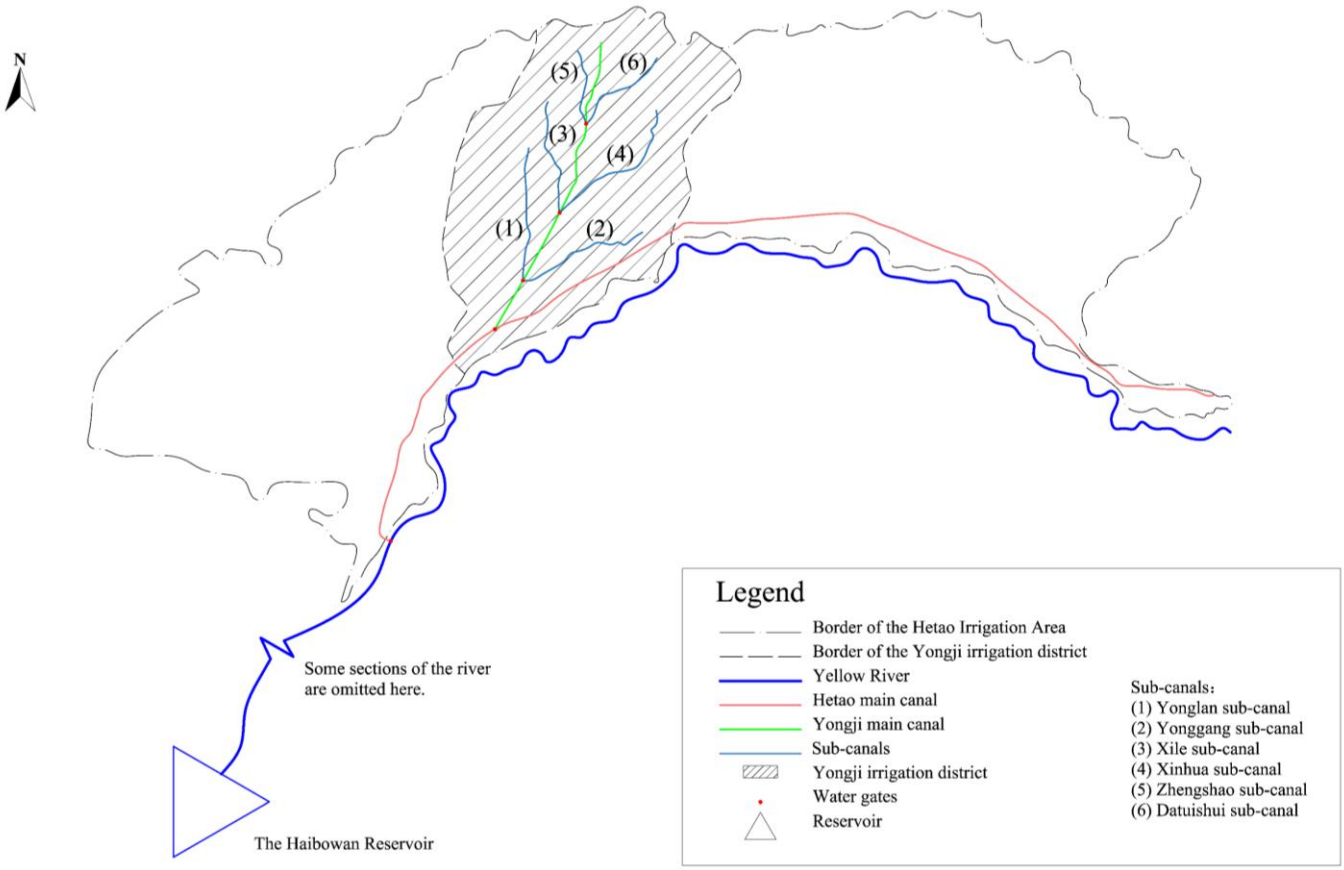

Figure 3. Overview of the Yongji Irrigation District and the Hetao Irrigation Area.

2.4. Data Preparation

In this study, the computational period for each year corresponds to the crop growing season, extending from 6 April to 12 September. A daily time step is adopted, yielding a total of 160 computation intervals per year. The dataset covers the period from 2001 to 2020, comprising 20 consecutive years of observations. Data from 2001 to 2010 are employed for parameter calibration of the BT model, whereas data from 2011 to 2020 are reserved for independent model validation.

The data on canal engineering parameters, irrigation area, maximum water supply, and residual lump-sum water quota used in this study are obtained from the Hetao Irrigation Area Administration Bureau. This study assumes that all irrigation areas in the Yongji Irrigation District are planted with three crops: wheat, corn, and sunflower, and no

other crops are considered. The planting area of each crop is based on the average planting area of the corresponding crop in the Yongji Irrigation District over the five years from 2016 to 2020.

2.5. Performance Evaluation Indicators

To evaluate the canal scheduling performance of each model, the following indicators are used to conduct a comparative analysis of the performance during the verification period.

The sum of the water shortage index of all sub-canals is the most important indicator for evaluating canal scheduling performance, as it directly reflects the degree to which water demand is met.

$$SWSI_y = \frac{100}{T}\sum_{t=1}^{T}\sum_{\substack{k=1 \\ D_{y,t,k}>0}}^{K}\left(\frac{R_{y,t,k}-D_{y,t,k}}{D_{y,t,k}}\right)^2 \tag{30}$$

The canal system's water loss rate reflects the proportion of water lost during the canal water conveyance process.

$$TWLR_y = \frac{\sum_{t=1}^{T} TWL_{y,t}}{\sum_{t=1}^{T} MRG_{y,t}} \tag{31}$$

The utilization rate of the initial lump-sum water quota reflects the degree to which water sources are utilized.

$$URILSWQ_y = \frac{\sum_{t=1}^{T} MRG_{y,t}}{ILSWQ_y} \tag{32}$$

3. Results

3.1. The Canal Scheduling Rules of the BT Model

Figure 4 illustrates the temporal evolution of the *TRLSWQ* for each period. As shown in the figure, from April to September, during the progression of the summer and autumn irrigation canal scheduling, the *TRLSWQ* exhibits a clear decreasing trend, declining from 3.96×10^8 m^3 to 0.03×10^8 m^3. Figure 5a further indicates that the *TWV* associated with each sub-canal also decreases progressively over the scheduling period. Among them, the Xinhua sub-canal has the highest *TWV*, decreasing from 4.16×10^8 m^3 on 6 April to 0.69×10^8 m^3 on 12 September, whereas the Datuishui sub-canal has the lowest *TWV*, dropping from 3.46×10^8 m^3 on April 6th to 0.11×10^8 m^3 on 12 September. The period-by-period decline in both *TRLSWQ* and *TWV* is consistent with the general pattern of irrigation districts, in which the total required irrigation water volume gradually diminishes over time. Also, the *TRLSWQ* and *TWV* lines all lie within the upper and lower envelope bounds of the actual *RLSWQ* in 2001~2010. Figure 5b shows that, in years with abundant precipitation (e.g., 2008), the *RLSWQ* trajectories predominantly fall below the corresponding *TRLSWQ* and *TWV* values for each period.

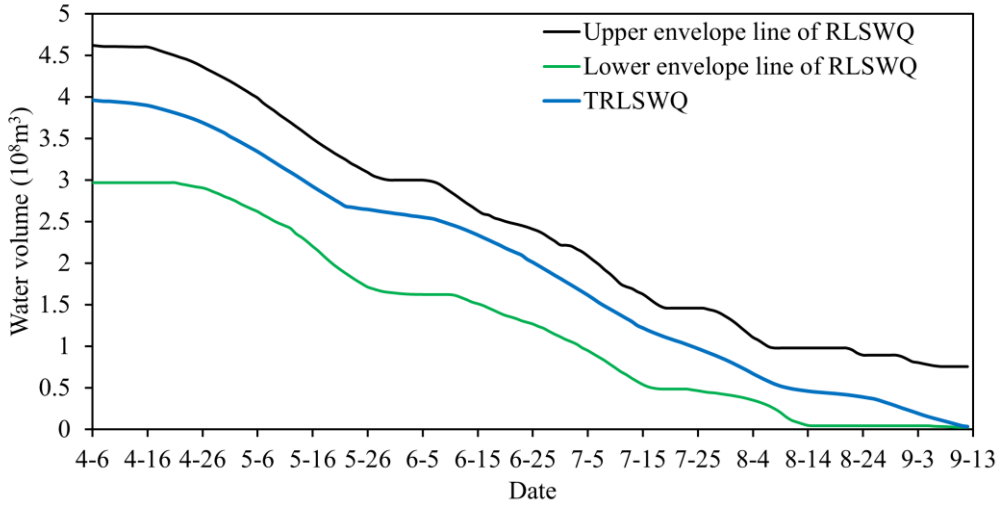

Figure 4. The target residual lump-sum water quota (*TRLSWQ*) obtained from the "Bi-level, Two-stage" dynamically updated canal scheduling model's calibration, as well as the upper and lower envelope lines of the residual lump-sum water quota (*RLSWQ*) process corresponding to the actual canal schedule process from 2001 to 2010. Note: The dates in the figure are in the "Month-Day" format.

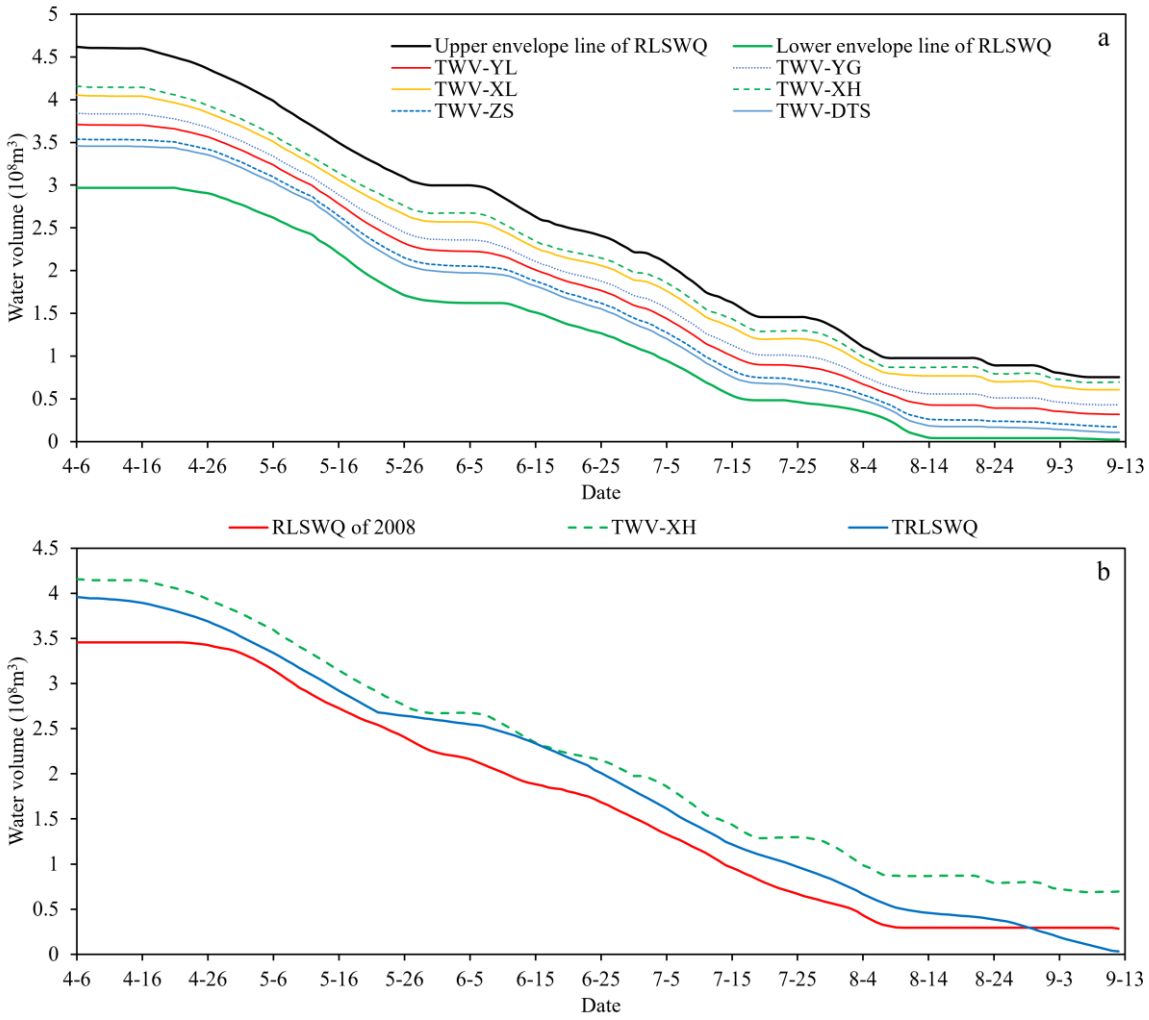

Figure 5. (**a**) The threshold water volume (*TWV*) of each sub-canal obtained from the "Bi-level, Two-stage" dynamically updated canal scheduling model's calibration, as well as the upper and lower envelope lines of the residual lump-sum water quota (*RLSWQ*) process corresponding to the actual

canal schedule process from 2001 to 2010. (**b**) The *RLSWQ* process in 2008, the *TWV* of the Xinhua (XH) sub-canal, and the target residual lump-sum water quota (*TRLSWQ*). Note: (1) Abbreviation of sub-canals: Yonglan (YL), Yonggang (YG), Xile (XL), Xinhua (XH), Zhengshao (ZS), and Datuishui (DTS). (2) The dates in the figure are in the "Month-Day" format.

3.2. Representative Canal Schedule Process and Overall Canal Scheduling Performance

Figure 6 presents five representative water delivery schedules—starting on 6 April, 1 May, 1 June, 1 July, and 1 August—for two representative years, 2013 and 2016, as generated by the CC model and the BT model. In these panels, red circles indicate the initial time steps of the decisions made by the CC model. Figure 7 further illustrates the water delivery processes at the intake of the Yongji main canal for all three models from 2001 to 2020. As shown in Figure 7, the seasonal characteristics of irrigation demand produce a broadly consistent trend across the three delivery processes, each displaying a distinct bimodal pattern associated with the summer and autumn irrigation periods. Except for 2013, the CC model exhibits systematic under-delivery during peak demand periods, during which the gray line lies substantially above the green line. Using 2013 as a representative case, Figure 8 presents the water delivery processes of six sub-canals for the three models. The aggregated sub-canal delivery patterns closely mirror those of the Yongji main canal, with peak deliveries concentrated in May and July of that year.

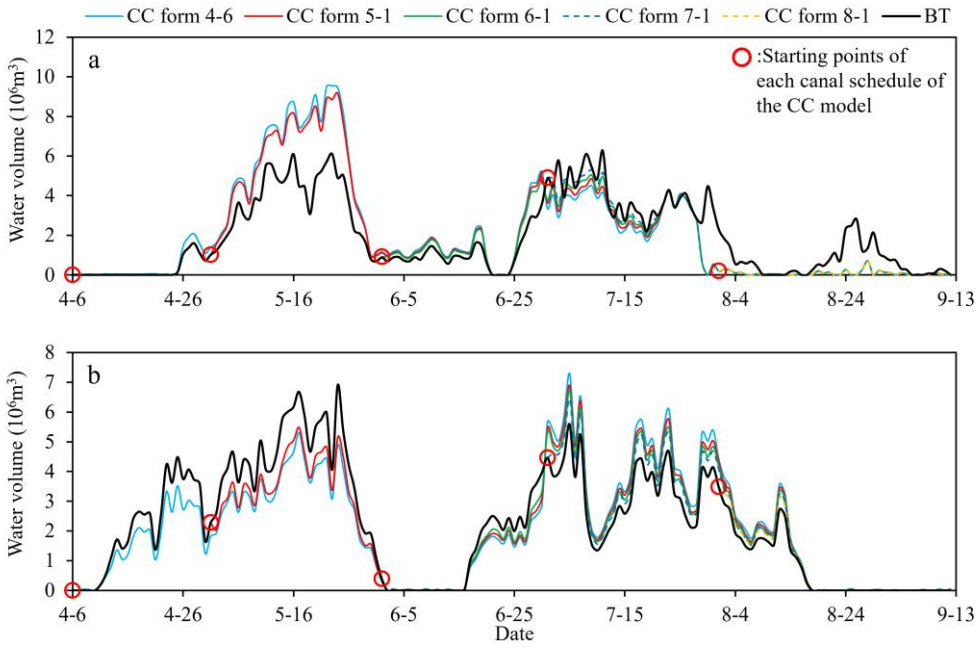

Figure 6. Five representative main canal scheduling decision-making processes derived by the conventional dynamically updated canal scheduling (CC) model on 6 April, 1 May, 1 June, 1 July, and 1 August in (**a**) 2013 and (**b**) 2016, and the main canal scheduling process of the whole growth stage of the "Bi-level, Two-stage" dynamically updated canal scheduling (BT) model. Note: (1) The red circles in the figure indicate the starting points of the five selected representative decision-making processes of the CC model. (2) The dates in the figure are in the "Month-Day" format.

As shown in Table 2, the multi-year average values of *SWSI* for the OC model, BT model, and CC model are 22.92, 31.44, and 40.81, respectively. Compared with the CC model, the value of the BT model is reduced by 22.9%, which is significantly better than the CC model and closer to the OC model (Due to the small sample size and non-normal distribution of the data, the Wilcoxon signed-rank test was employed. The results confirmed that the difference in *SWSI* between the BT and CC models was statistically

significant, with W = 0.0, p = 0.0051, and r = 0.8864). For the multi-year average value of *TWLR*, the OC model is 2.80%, the BT model is 2.99%, and the CC model is 3.10%. The water loss of the CC model is slightly higher. For the multi-year average value of *URILSWQ*, the OC model is 93.66%, the BT model is 92.82%, and the CC model is 89.32%. Therefore, the BT model's utilization effect of the residual lump-sum water quota also falls between the OC model and the CC model.

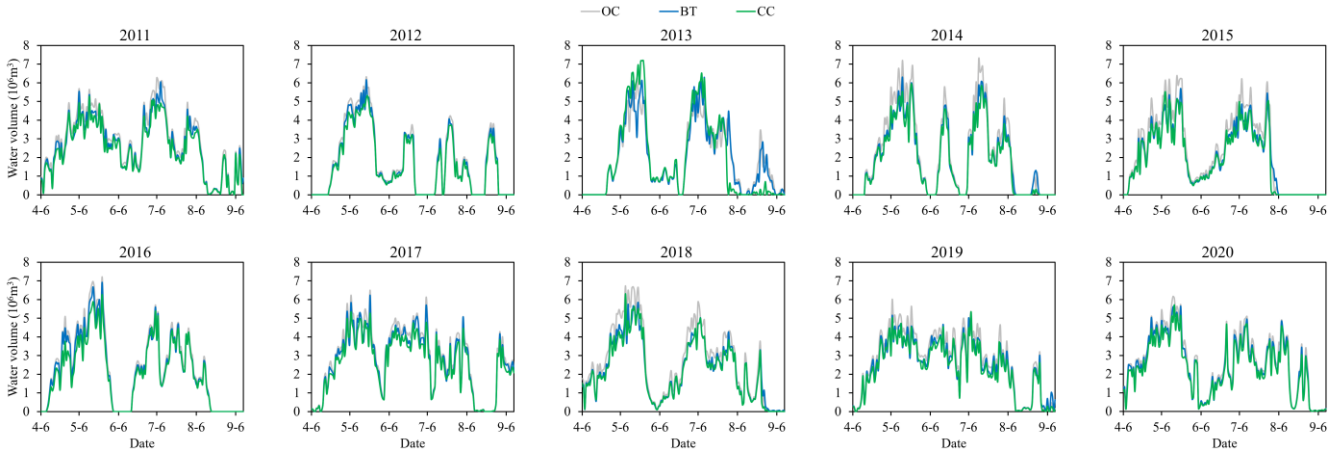

Figure 7. Comparison of main canal scheduling processes among the optimal static canal scheduling (OC) model, the "Bi-level, Two-stage" dynamically updated canal scheduling (BT) model, and the conventional dynamically updated canal scheduling (CC) model in the years 2011 to 2020. Note: The dates in the figure are in the "Month-Day" format.

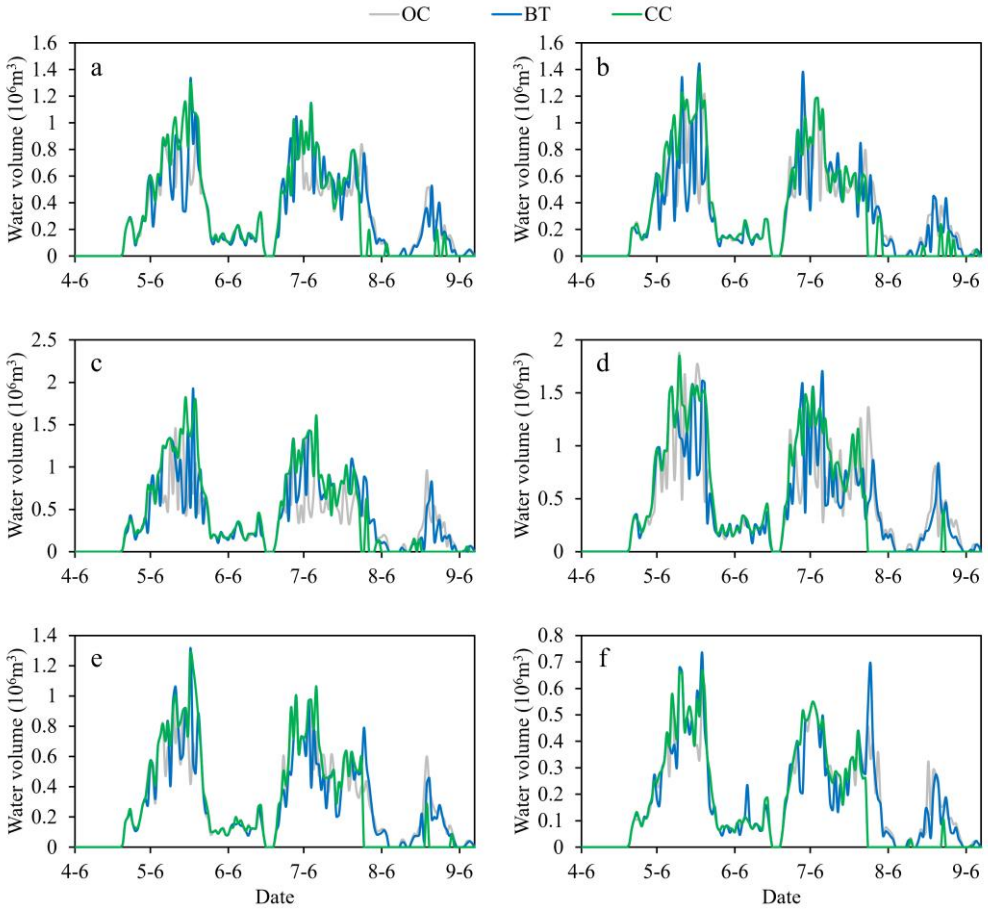

Figure 8. Comparison of sub-canals' scheduling processes among the optimal static canal scheduling (OC) model, the "Bi-level, Two-stage" dynamically updated canal scheduling (BT) model, and

the conventional dynamically updated canal scheduling (CC) model in the year 2013. Among them: (**a**) Yonglan, (**b**) Yonggang, (**c**) Xile, (**d**) Xinhua, (**e**) Zhengshao, and (**f**) Datuishui. Note: The dates in the figure are in the "Month-Day" format.

Table 2. Multi-year average values of canal scheduling performance evaluation indicators for the optimal static canal scheduling (OC) model, the "Bi-level, Two-stage" dynamically updated canal scheduling (BT) model, and the conventional dynamically updated canal scheduling (CC) model during the years 2011 to 2020.

Indicator	The OC Model	The BT Model	The CC Model
The sum of the water shortage index (*SWSI*)	22.92 ± 14.15	31.44 ± 17.07	40.81 ± 30.64
The canal system's water loss rate (*TWLR*)	2.80 ± 0.21%	2.99 ± 0.14%	3.10 ± 0.18%
The utilization rate of the initial lump-sum water quota (*URILSWQ*)	93.66 ± 2.93%	92.82 ± 2.91%	89.32 ± 2.80%

3.3. Analysis of the Canal Scheduling Strategy of the BT Model

As shown in the comparison of the 10-year series for the verification period in Section 3.2, the BT model outperforms the CC model in overall canal scheduling performance. To analyze the causes of the differences in canal scheduling and further explore the mechanism by which the BT model achieves better results in dynamically updated canal scheduling, this section selects two representative scenarios for analysis: scenarios with underestimated and overestimated forecast precipitation in earlier periods.

3.3.1. Scenario with Underestimated Forecast Precipitation in Earlier Periods

Figure 9 compares the temporal variation in the flow rate of the water delivery processes of the main canal produced by the BT model, the CC model, and the observed. As shown in Figure 9a,b, the BT model produces lower flow peaks than the CC model from April through July, but higher peaks from August through September. In terms of the temporal distribution of delivered water, the BT model achieves a more balanced allocation across the irrigation season. By deliberately constraining early-season deliveries, the BT model preserves the remaining lump-sum water-use quota, thereby preventing severe late-season shortages. In contrast, the CC model maintains relatively high deliveries in the early periods, which exhausts the available quota and leads to pronounced water deficits in the later stages.

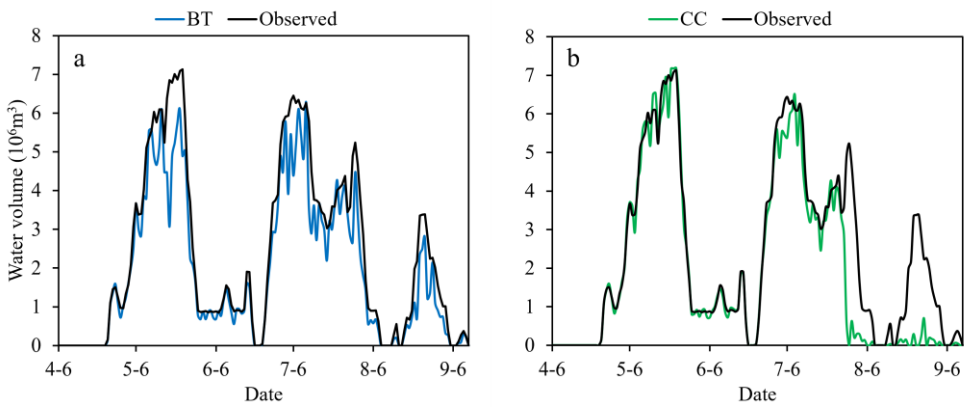

Figure 9. Main canal scheduling process of (**a**) the "Bi-level, Two-stage" dynamically updated canal scheduling (BT) model and (**b**) the conventional dynamically updated canal scheduling (CC) model

in 2013, and the observed process in 2013. Note: The dates in the figure are in the "Month-Day" format.

Figure 10a compares the temporal variation in flow rate of the CC model on 6 April 2013, and the all-period canal scheduling decision of the BT model in 2013, as well as the forecast precipitation process at the beginning of 6 April and the observed precipitation process. Figure 10b illustrates the magnitude relationship between the *RLSWQ* of the BT model and the typical *TWV* in each period throughout the entire canal scheduling process. It can be seen from Figure 10a that the forecast precipitation is underestimated in earlier periods of the canal schedule (from April to mid-July) and overestimated in later periods (from mid-July to September), which results in the water allocation volume of the CC model being significantly higher in earlier periods and lower in later periods. Figure 10b shows that during the canal scheduling process in 2013, compared to the highest line of *TWV* of the XH sub-canal and the lowest line of *TWV* of the DTS sub-canal, the *RLSWQ* was lower than the *TWV* in most periods. This magnitude relationship enabled the BT model to activate the hedging mechanism, thereby avoiding the severe water shortage in later periods caused by the depletion of the *RLSWQ* in earlier periods.

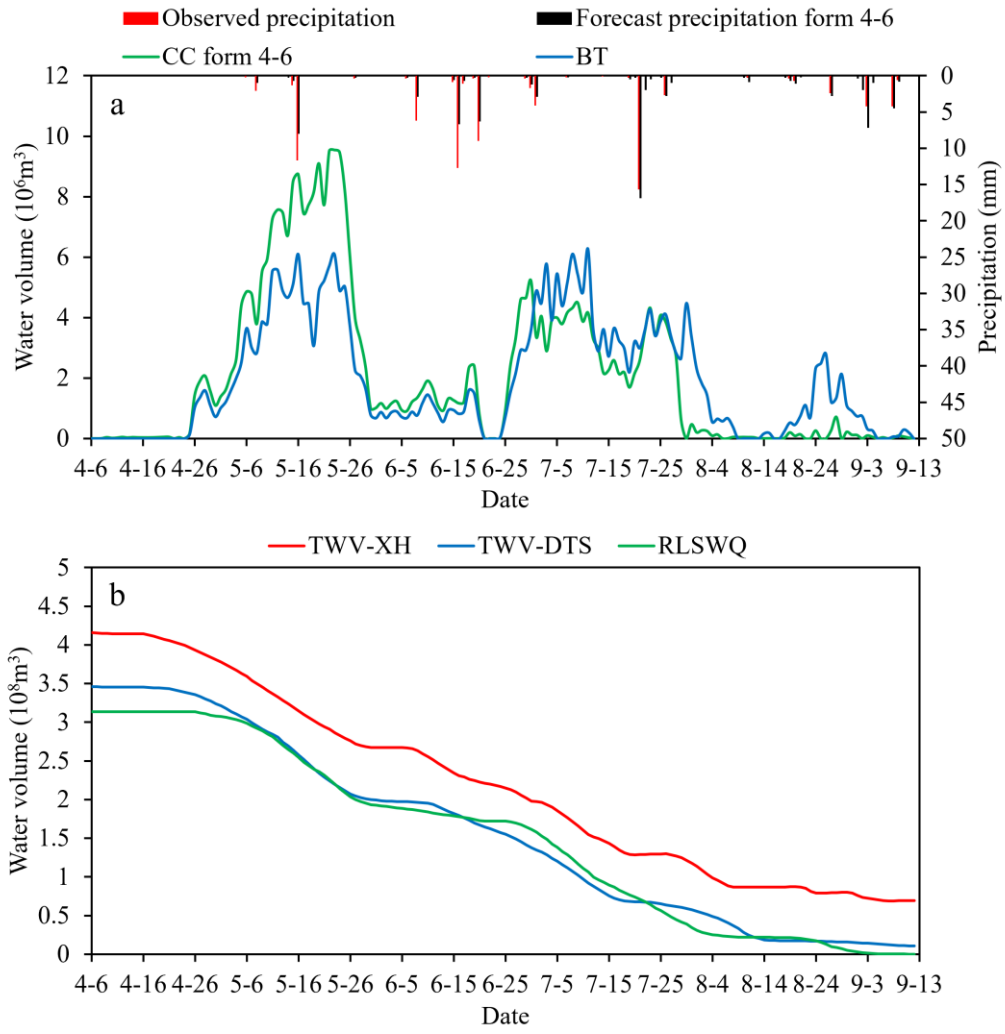

Figure 10. (**a**) The canal scheduling decision made by the conventional dynamically updated canal scheduling (CC) model on 6 April 2013, and the all-period canal scheduling decision of the "Bi-level, Two-stage" dynamically updated canal scheduling (BT) model in 2013, as well as the forecast precipitation process at the beginning of April 6th and the observed precipitation process. (**b**) The residual lump-sum water quota (*RLSWQ*) process of the BT model in 2013 and the threshold water

volume (*TWV*) process of the Xinhua (XH) and Datuishui (DTS) sub-canals. Note: The dates in the figure are in the "Month-Day" format.

3.3.2. Scenario with Overestimated Forecast Precipitation in Earlier Periods

Figure 11 compares the canal scheduling processes of the BT model, the CC model, and the observed canal scheduling process in 2016, respectively. In 2016, the actual situation was that the maximum residual lump-sum water quota during the growth stage was relatively sufficient, with a water volume of 4.33×10^8 m^3. After the completion of canal scheduling in 2016, the *SWSI* of the OC model was 0.85, the corresponding value of the BT model was 7.06, and that of the CC model was 17.16. This result indicates that the OC model had almost no water shortage, the BT model had a low degree of water shortage throughout the entire growth stage, while the CC model had a significant water shortage.

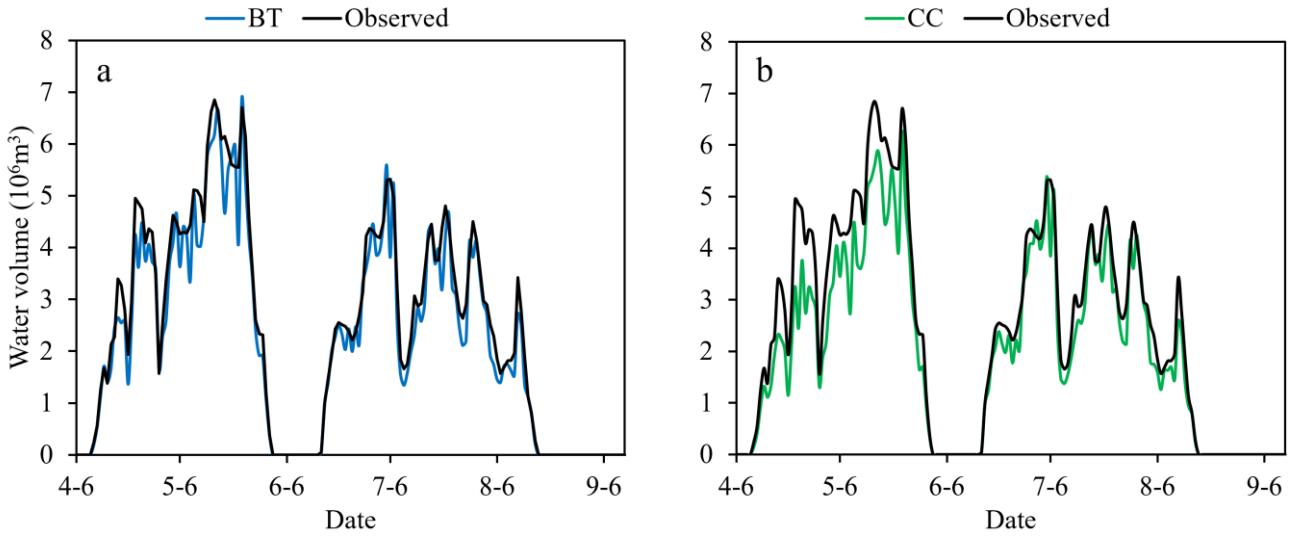

Figure 11. Main canal scheduling process of (**a**) the "Bi-level, Two-stage" dynamically updated canal scheduling (BT) model and (**b**) the conventional dynamically updated canal scheduling (CC) model in 2016, and the observed process in 2016. Note: The dates in the figure are in the "Month-Day" format.

In the canal scheduling during the growth stage of this year, the total water allocation volume of the CC model was 3.25×10^8 m^3, while that of the BT model was 3.54×10^8 m^3, indicating a relatively low utilization rate of the residual lump-sum water quota for the CC model. Figure 11a shows that the canal scheduling process of the BT model was close to the observed process in 2016. In contrast, Figure 11b shows that the CC model had less water allocation in earlier periods, and its canal scheduling process was closer to the observed process in 2016 in later periods.

Figure 12a presents a comparison of the initial decision-making canal scheduling process line of the CC model and that of the BT model in 2016, as well as the forecast precipitation process at the beginning of 6 April and the observed precipitation process. As shown in Figure 12a, the canal scheduling process of the CC model exhibits a phenomenon where the water allocation volume is significantly lower in earlier periods and higher in later periods. This characteristic of the process may be due to the forecast precipitation being overestimated in earlier periods (from April to mid-July) and underestimated in later periods (from mid-July to September). Nevertheless, the canal scheduling process of the BT model is close to the observed process. It does not restrict water volume in earlier periods, even though the forecast precipitation is overestimated in earlier periods.

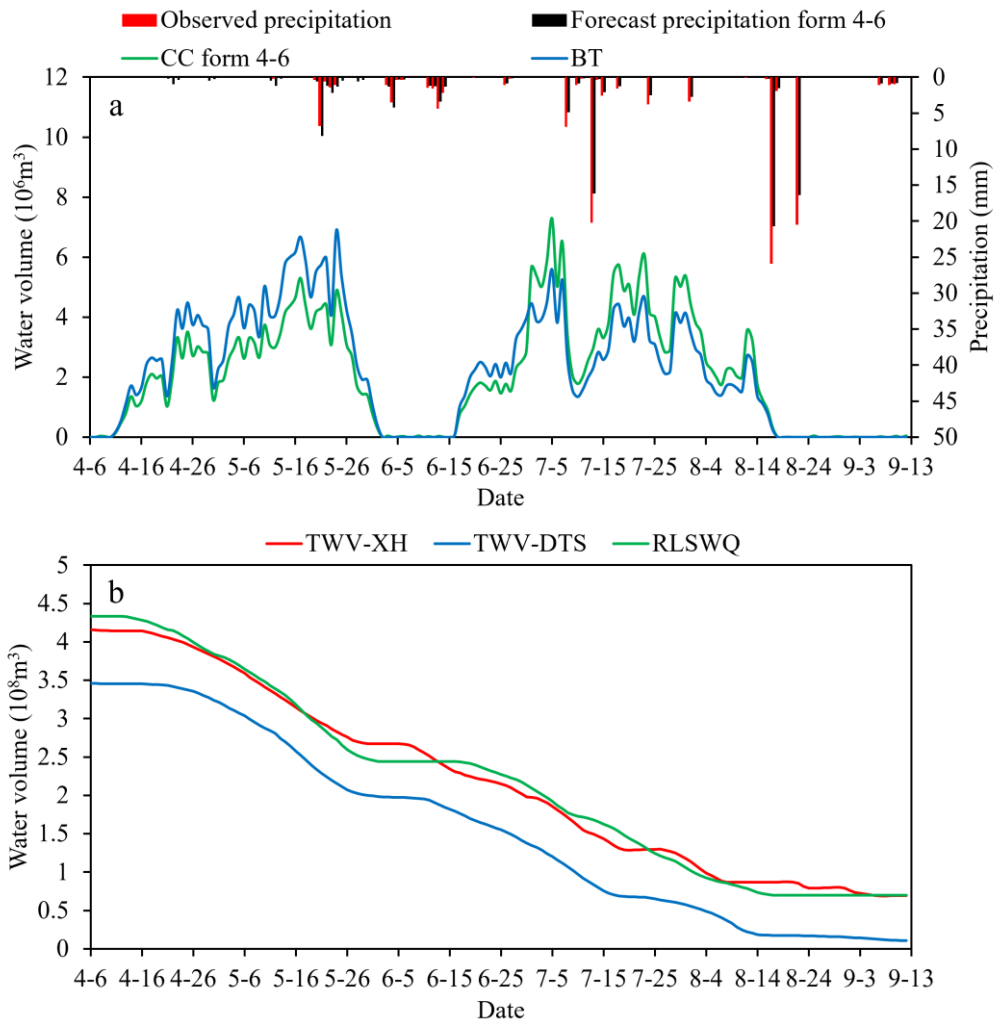

Figure 12. (**a**) The canal scheduling decision made by the conventional dynamically updated canal scheduling (CC) model on 6 April 2016, and the all-period canal scheduling decision of the "Bi-level, Two-stage" dynamically updated canal scheduling (BT) model in 2016, as well as the forecast precipitation process at the beginning of 6 April and the observed precipitation process. (**b**) The residual lump-sum water quota (*RLSWQ*) process of the BT model in 2016 and the threshold water volume (*TWV*) process of the Xinhua (XH) and Datuishui (DTS) sub-canals. Note: The dates in the figure are in the "Month-Day" format.

Figure 12b shows that the *RLSWQ* of the BT model is higher than the lowest *TWV*–the *TWV* of the DTS sub-canal, and in most periods, it is also higher than the highest one–the *TWV* of the XH sub-canal. During the canal scheduling process in 2016, the *RLSWQ* of the BT model was not lower than the *TWV* from April to late May, allowing it to meet the water demand in this period as much as possible without implementing restricted water allocation. From late May to mid-June, although the *RLSWQ* was lower than the *TWV* corresponding to some sub-canals, the water demand was very small at this time, which had little impact on the canal scheduling performance. From late June to the end of the growth stage, the *RLSWQ* was generally not lower than the *TWV*, and the canal schedule was also implemented to meet water demand as much as possible. Therefore, during the canal scheduling process of the growth stage in 2016, due to the relatively large maximum residual lump-sum water quota, the BT model met the water demand as much as possible, avoided unnecessary restrictions caused by forecast errors, and thus improved the utilization rate of the *RLSWQ* and the overall performance of the canal scheduling.

4. Discussion

The previous section compared and analyzed the canal scheduling performance of the OC model, the CC model, and the BT model, respectively. From a comprehensive perspective that includes the richness of information sources, the required lead time for forecast information, the transparency of canal scheduling decisions, and overall performance, the BT model proposed in this study offers advantages such as utilizing diverse information sources, having low requirements for forecast lead time, employing clear canal scheduling rules, and achieving strong canal scheduling performance.

The OC and CC models impose stringent requirements on both the accuracy of forecast information and the length of the forecast lead time. Specifically, the OC model assumes perfectly accurate hydrometeorological forecasts with a sufficiently long lead time—long enough to cover the entire canal scheduling horizon and even the full crop growth period [6,38]. For example, Fan et al. [38] generated canal-scheduling plans for the wheat greening stage in 2017, the wheat grain-filling stage in 2018, and the wheat greening stage in 2019 in the Bojili Irrigation District, Shandong Province, China; these plans required precise forecasts of crop water demand 20, 10, and 15 days in advance, respectively. Zhou et al. [6] developed a canal scheduling plan for autumn irrigation during the non-growing season in the Hetao Irrigation District, which required hydrometeorological forecasts extending up to two months and assumed complete accuracy. For the CC model, the decision in the first period is identical to that of the OC model and therefore requires the same long forecast lead time. However, as the canal scheduling process evolves and decisions are updated dynamically, the required forecast lead time for subsequent periods gradually decreases.

In contrast, the BT model can effectively integrate two categories of information within the irrigation district—extensive historical canal scheduling records (*TRLSWQ* and *TWV*) and inflow–demand forecast data—to generate robust delivery schedules. Because it updates decisions dynamically on a period-by-period basis, and can even operate with daily updates, the BT model requires only short-term hydrometeorological forecasts, typically with a lead time of just one day.

The BT model explicitly defines the canal scheduling rules through two key elements: the *TRLSWQ* of the water source and the *TWV* assigned to each canal. To the best of the authors' knowledge, no comparable studies have been reported in the field of irrigation canal scheduling to date [10]. A central innovation of this work is the establishment of a hedging-trigger rule based on the relationship between the *RLSWQ* and the *TWV* at the beginning of each period (Figure 5). Specifically, hedging is activated when the *RLSWQ* falls below the corresponding threshold, resulting in a reduction in the delivery volume at the canal inlet; conversely, hedging is terminated when the *RLSWQ* exceeds the threshold, and water is allocated according to demand. The positions of the *TWV* curves optimized by the BT model for different sub-canals vary. The main reason is that the water demand processes of different sub-canals are distinct, which in turn leads to differences in their contributions to the upper-level objective function value in the upper-level model during the calibration process of the BT model. Water shortages in some sub-canals (e.g., XH) will have a greater impact on the overall objective, thus resulting in a higher *TWV* position; in contrast, the situation is reversed for sub-canals with a lower *TWV* position (e.g., DTS). In addition, Figure 4 provides reference values of *TRLSWQ* for each period by matching historical patterns of water availability and irrigation demand. In the domain of reservoir operation, extensive research has explored storing water in advance to mitigate the risk of severe shortages later in the season [39–43]. In these studies, hedging is typically triggered when certain diagnostic indicators fall below their respective thresholds. These indicators may include the sum of current reservoir storage and inflow (i.e., water availability) [35], a drought frequency index [44], or a drought limit water level [45]. In general

terms, the "hedging" concept can also be applied to all water supply systems with similar characteristics when addressing the issue of allocating water resources across different periods to maximize overall benefits as much as possible. Unlike many two-stage reservoir operation models that focus solely on deriving the *TWV* within hedging rules, the present study employs a Bi-level programming framework to jointly determine the *TRLSWQ* for each period and the *TWV* in a coordinated manner [46,47].

In contrast, both the CC and OC models determine whether and to what extent water allocation should be reduced in each period by solving complex optimization models, which requires them to be equipped with corresponding computing power at all times. Additionally, the range of the resulting decisions of the two models cannot be predicted in advance, leading to significant limitations in real-world applications. The BT model, by comparison, provides transparent and operationally interpretable scheduling rules, thereby enhancing the practicality and traceability of irrigation canal scheduling decisions.

From the perspective of canal scheduling performance in the case study, the BT model performs between the OC model and the CC model. Accurate forecasts are a prerequisite for the OC model to achieve optimal canal scheduling results. Conducting canal scheduling using dynamically updated information is an effective approach to modifying static canal scheduling plans under forecast errors, thereby guiding actual canal scheduling. For example, Puig et al. [29] integrated real-time meteorological data from on-site weather stations and utilized low-cost RGB cameras to monitor the dynamic changes in crop green canopy coverage continuously, enabling them to update version 6 of the AquaCrop model dynamically, resulting in an approximate 32% reduction in the recommended irrigation amount during the wheat-growing season. However, all dynamically updated canal scheduling models have the problem that, as forecast accuracy decreases, canal scheduling performance deviates more from optimal performance. Among relevant studies, Wang and Cai [30] found that formulating irrigation plans using accurate weather forecasts for one week, two weeks, and the entire irrigation season in dry years could increase net profits by 5%, 16%, and 22%, respectively. The BT model addresses the issue of the rapidly diminishing marginal returns of forecasts as the lead time extends by referencing both forecast information and the target residual lump-sum water quota simultaneously. It prevents scenarios where an underestimation of the precipitation forecast in earlier periods leads to excessive increases in water allocation for the current period, resulting in no available water for allocation in later periods (Figure 9). Similarly, it avoids situations where an overestimation of the precipitation forecast in earlier periods leads to excessive reductions in water allocation, resulting in a water surplus that fails to meet the demand during those periods. (Figure 11).

The BT model does not necessarily outperform the CC model in terms of canal scheduling performance under all scenarios. That is because whether the BT model can correctly control the canal scheduling process hinges on the values of *TRLSWQ* and *TWV*, which in turn depend on the representativeness of the historical data used for calibration. If the values of *TRLSWQ* and *TWV* are excessively high, it may lead to unnecessary restrictions and artificially create water shortage incidents. Similarly, if their values are too low, the *RLSWQ* will be used up prematurely, resulting in severe water shortage in the later period. Once there is a significant deviation in the parameters, even with accurate forecast values, the deviation in the canal scheduling process cannot be avoided. Nevertheless, this issue can be mitigated by utilizing medium- and long-term hydrometeorological forecasts to optimize the target residual lump-sum water quota dynamically.

5. Conclusions

This study proposes a dynamically updated canal system scheduling model that is based on the target residual lump-sum water quota at the beginning of each period and hydrometeorological forecast information. A case study is conducted using the canal scheduling for summer and autumn irrigation in the Yongji main canal and its six sub-canals in the Yongji Irrigation District of Hetao Irrigation Area, Inner Mongolia, China. The main conclusions are as follows:

(1) A dynamically updated canal system scheduling strategy is proposed, which incorporates both the target residual lump-sum water quota at the beginning of each period and hydrometeorological forecast information. This strategy addresses the limitations of current strategies, which rely solely on water availability and crop water demand forecasts. Specifically, it mitigates issues such as excessive water allocation in earlier periods caused by underestimated precipitation forecasts, which can lead to water shortages in later periods, or excessive restriction in earlier periods caused by overestimated precipitation forecasts, which can lead to water wastage in later periods. This strategy encourages irrigation district managers to thoroughly examine historical canal system scheduling data and plan the canal schedule based on established rules, enabling them to implement water allocation restriction measures in a timely and appropriate manner.

(2) Canal scheduling rules for the canal system in the Yongji Irrigation District are provided, including the target and threshold water volume at the beginning of each period, and the degree of restriction applied when hedging is triggered. Compared to the conventional model, the rules reduced the sum of the water shortage index of sub-canals by 22.9% and increased the utilization rate of the residual lump-sum water quota by 3.9%.

(3) The proposed dynamically updated canal scheduling model offers several advantages, including the effective use of diverse information sources, minimal lead time requirements for forecast information, clear canal scheduling rules, and achieving good performance in optimizing canal scheduling.

The "Bi-level, Two-stage" model for dynamically updated canal-system scheduling, established in this study, provides strong theoretical guidance and practical value for efficient canal scheduling in irrigation districts. In future research, it can be combined with theories such as machine learning and intelligent forecasting and control, showing broad prospects.

Author Contributions: M.Y., writing—original draft preparation, software, validation; F.W., formal analysis, writing—review and editing; L.C., writing—review and editing; Y.L., writing—review and editing; X.Z., writing—review and editing, supervision; T.H., conceptualization, formal analysis, writing—review and editing, supervision. All authors have read and agreed to the published version of the manuscript.

Funding: This research was funded by the Key Water Conservancy Research Project of Hubei Province (HBSLKY202409) and the National Natural Science Foundation of China (52179022).

Institutional Review Board Statement: Not applicable.

Data Availability Statement: The data presented in this study are available upon request from the corresponding author.

Conflicts of Interest: Author Yong Liu was employed by the company China Three Gorges Corporation. The remaining authors declare that the research was conducted in the absence of any commercial or financial relationships that could be construed as a potential conflict of interest.

Appendix A

Table A1. List of crop coefficients.

Growth Period		Crop		
Start Date	**End Date**	**Wheat**	**Corn**	**Sunflower**
6 April	10 April	0.40	/	/
11 April	20 April	0.50	0.40	/
21 April	30 April	0.55	0.40	/
1 May	10 May	0.60	0.45	0.30
11 May	20 May	0.70	0.50	0.30
21 May	31 May	0.85	0.50	0.30
1 June	10 June	0.90	0.60	0.30
11 June	20 June	1.00	0.70	0.40
21 June	30 June	1.00	0.80	0.50
1 July	10 July	0.90	1.00	0.70
11 July	20 July	0.70	1.00	0.90
21 July	31 July	0.50	1.00	1.00
1 August	10 August	/	0.90	1.10
11 August	20 August	/	0.90	1.10
21 August	31 August	/	0.75	0.90
1 September	12 September	/	0.50	0.80

Note./indicates the non-growing period.

Table A2. List of upper (SWU) and lower (SWL) limits of the suitable soil moisture content.

Month	Wheat		Corn		Sunflower	
	SWU	**SWL**	**SWU**	**SWL**	**SWU**	**SWL**
4	125	86	121	83	/	/
5	187	86	182	83	161	74
6	218	129	195	125	173	110
7	218	150	212	137	187	121
8	/	/	212	146	187	129
9	/	/	212	146	187	129

Note. (1)/indicates the non-growing period. (2) Unit: mm.

References

1. Food and Agriculture Organization of the United Nations (FAO). *The State of the World's Land and Water Resources for Food and Agriculture—Systems at Breaking Point*; FAO: Rome, Italy, 2021; p. 11.
2. Kamrani, K.; Roozbahani, A.; Shahdany, S.M.H. Using Bayesian networks to evaluate how agricultural water distribution systems handle the water-food-energy nexus. *Agric. Water Manag.* **2020**, *239*, 12. https://doi.org/10.1016/j.agwat.2020.106265.
3. Lakhiar, I.A.; Yan, H.; Zhang, C.; Wang, G.; He, B.; Hao, B.; Han, Y.; Wang, B.; Bao, R.; Syed, T.N.; et al. A Review of Precision Irrigation Water-Saving Technology under Changing Climate for Enhancing Water Use Efficiency, Crop Yield, and Environmental Footprints. *Agriculture* **2024**, *14*, 38. https://doi.org/10.3390/agriculture14071141.
4. Mancosu, N.; Snyder, R.L.; Kyriakakis, G.; Spano, D. Water Scarcity and Future Challenges for Food Production. *Water* **2015**, *7*, 975–992. https://doi.org/10.3390/w7030975.
5. Liao, X.; Mahmoud, A.; Hu, T.; Wang, J. A novel irrigation canal scheduling model adaptable to the spatial-temporal variability of water conveyance loss. *Agric. Water Manag.* **2022**, *274*, 107961. https://doi.org/10.1016/j.agwat.2022.107961.
6. Zhou, S.; Hu, T.; Zhu, R.; Wu, F.; Wang, X. A bilevel modeling approach for optimizing irrigation canal scheduling under a hierarchical institutional arrangement. *Agric. Water Manag.* **2023**, *284*, 108322. https://doi.org/10.1016/j.agwat.2023.108322.
7. Haque, M.A.; Najim, M.M.M.; Lee, T.S. Modeling irrigation water delivery schedule for rice cultivation in East Coast Malaysia. *Trop. Agric. Res.* **2004**, *16*, 204–213.

8. Mishra, A.; Singh, R.; Raghuwanshi, N.S. Alternative delivery scheduling for improved canal system performance. *J. Irrig. Drain. Eng.* **2002**, *128*, 244–248. https://doi.org/10.1061/(ASCE)0733-9437(2002)128:4(244).
9. Suryavanshi, A.R.; Reddy, J.M. Optimal operation schedule of irrigation distribution-systems. *Agric. Water Manag.* **1986**, *11*, 23–30. https://doi.org/10.1016/0378-3774(86)90033-8.
10. Zhou, K.; Fan, Y.; Gao, Z.; Chen, H.; Kang, Y. Research progress on operation control and optimal scheduling of irrigation canal systems. *Irrig. Drain.* **2025**, *74*, 861–879. https://doi.org/10.1002/ird.3028.
11. Anwar, A.A.; Bhatti, M.T.; de Vries, T.T. Canal Operations Planner. I: Maximizing Delivery Performance Ratio. *J. Irrig. Drain. Eng.* **2016**, *142*, 12. https://doi.org/10.1061/(ASCE)IR.1943-4774.0001091.
12. Fan, Y.; Yang, M.; Zhou, K.; Gao, Z.; Zhang, W.; Guo, B.; Zhang, X. Irrigation Scheduling and Water Distribution Evaluation Model Based on Water Supply Flow Rate. *J. Irrig. Drain. Eng.* **2025**, *151*, 9. https://doi.org/10.1061/JIDEDH.IRENG-10466.
13. Fan, Y.; Chen, H.; Gao, Z.; Fang, B.; Liu, X. A Model Coupling Water Resource Allocation and Canal Optimization for Water Distribution. *Water Resour. Manag.* **2023**, *37*, 1341–1365. https://doi.org/10.1007/s11269-023-03437-9.
14. Anwar, A.A.; de Vries, T.T.; Bhatti, M.T. Canal Operations Planner. II: Minimizing Inequity. *J. Irrig. Drain. Eng.* **2016**, *142*, 7. https://doi.org/10.1061/(ASCE)IR.1943-4774.0001092.
15. Santhi, C.; Pundarikanthan, N.V. A new planning model for canal scheduling of rotational irrigation. *Agric. Water Manag.* **2000**, *43*, 327–343. https://doi.org/10.1016/S0378-3774(99)00065-7.
16. Zhou, S.; Hu, T.; Zhu, R.; Huang, J.; Shen, L. A novel irrigation canal scheduling approach without relying on a prespecified canal water demand process. *J. Clean. Prod.* **2021**, *282*, 124253. https://doi.org/10.1016/j.jclepro.2020.124253.
17. Monem, M.J.; Namdarian, R. Application of simulated annealing (SA) techniques for optimal water distribution in irrigation canals. *Irrig. Drain.* **2005**, *54*, 365–373. https://doi.org/10.1002/ird.199.
18. Delgoda, D.; Malano, H.; Saleem, S.K.; Halgamuge, M.N. A novel generic optimization method for irrigation scheduling under multiple objectives and multiple hierarchical layers in a canal network. *Adv. Water Resour.* **2017**, *105*, 188–204. https://doi.org/10.1016/j.advwatres.2017.04.025.
19. Fan, Y.; Chen, H.; Gao, Z.; Wang, Y.; Xu, J. Optimal water distribution model of canals considering the workload of managers. *Irrig. Drain.* **2023**, *72*, 182–195. https://doi.org/10.1002/ird.2751.
20. Nguyen, D.C.H.; Ascough, J.C.; Maier, H.R.; Dandy, G.C.; Andales, A.A. Optimization of irrigation scheduling using ant colony algorithms and an advanced cropping system model. *Environ. Modell. Softw.* **2017**, *97*, 32–45. https://doi.org/10.1016/j.envsoft.2017.07.002.
21. Sun, Z.; Chen, J.; Han, Y.; Huang, R.; Zhang, Q.; Guo, S. An Optimized Water Distribution Model of Irrigation District Based on the Genetic Backtracking Search Algorithm. *IEEE Access* **2019**, *7*, 145692–145704. https://doi.org/10.1109/ACCESS.2019.2944148.
22. Wu, J.J.; Huang, R.; Fang, T.Y.; Han, Y. Multi-objective model of irrigation water distribution based on particle swarm optimization. 5Th International Conference on Water Resource and Environment. *IOP Conf. Ser. Earth Environ. Sci.* **2019**, *344*, 8. https://doi.org/10.1088/1755-1315/344/1/012087.
23. Du, Y.; Zhang, C.; Wei, R.; Cao, L.; Zhao, T.; Wang, W.; Hu, X. Multi-Objective Optimal Scheduling of Water Transmission and Distribution Channel Gate Groups Based on Machine Learning. *Agriculture* **2025**, *15*, 23. https://doi.org/10.3390/agriculture15131344.
24. Tian, G.; Lv, M.; Wang, M.; Qin, J.; Wang, Y.; Yu, J.; Yang, B. A novel water distribution model considering the dynamic coupling of canals and gates. *Comput. Electron. Agric.* **2025**, *236*, 20. https://doi.org/10.1016/j.compag.2025.110434.
25. Kang, S.; Hao, X.; Du, T.; Tong, L.; Su, X.; Lu, H.; Li, X.; Huo, Z.; Li, S.; Ding, R. Improving agricultural water productivity to ensure food security in China under changing environment: From research to practice. *Agric. Water Manag.* **2017**, *179*, 5–17. https://doi.org/10.1016/j.agwat.2016.05.007.
26. Zheng, H.; Hou, H.; Wu, J.; Tian, D.; Miao, P. Irrigation Schedule Optimization for Wheat and Sunflower Intercropping under Water Supply Restrictions in Inner Mongolia, China. *Atmosphere* **2024**, *15*, 19. https://doi.org/10.3390/atmos15050566.
27. Cai, X.; Hejazi, M.I.; Wang, D. Value of Probabilistic Weather Forecasts: Assessment by Real-Time Optimization of Irrigation Scheduling. *J. Water Resour. Plan. Manag.* **2011**, *137*, 391–403. https://doi.org/10.1061/(ASCE)WR.1943-5452.0000126.
28. Hejazi, M.I.; Cai, X.; Yuan, X.; Liang, X.; Kumar, P. Incorporating Reanalysis-Based Short-Term Forecasts from a Regional Climate Model in an Irrigation Scheduling Optimization Problem. *J. Water Resour. Plan. Manag.* **2014**, *140*, 699–713. https://doi.org/10.1061/(ASCE)WR.1943-5452.0000365.
29. Puig, F.; Garcia-Vila, M.; Soriano, M.A.; Rodriguez-Diaz, J.A. AquaCrop-IoT: A smart irrigation platform integrating real-time images and weather forecasting. *Comput. Electron. Agric.* **2025**, *235*, 13. https://doi.org/10.1016/j.compag.2025.110372.

30. Wang, D.; Cai, X. Irrigation Scheduling-Role of Weather Forecasting and Farmers' Behavior. *J. Water Resour. Plan. Manag.* **2009**, *135*, 364–372. https://doi.org/10.1061/(ASCE)0733-9496(2009)135:5(364).
31. Li, H.; Liu, P.; Guo, S.; Cheng, L.; Huang, K.; Feng, M.; He, S.; Ming, B. Deriving adaptive long-term complementary operating rules for a large-scale hydro-photovoltaic hybrid power plant using ensemble Kalman filter. *Appl. Energy* **2021**, *301*, 15. https://doi.org/10.1016/j.apenergy.2021.117482.
32. Zhang, L.; Feng, Z.; Yao, X.; Niu, W.; Wang, Y.; Mo, L. A multi-objective operation optimization method for dynamic control of reservoir water level in evolving flood season environments. *J. Hydrol.* **2024**, *643*, 17. https://doi.org/10.1016/j.jhydrol.2024.131940.
33. Maass, A.; Hufschmidt, M.M.; Dorfman, R.; Thomas, H.A., Jr.; Marglin, S.A.; Fair, G.M. *Design of Water-Resources Systems: New Techniques for Relating Economic Objectives, Engineering Analysis, and Government Planning*; Harvard University Press: Cambridge, UK, 1962; p. 638.
34. Draper, A.J.; Lund, J.R. Optimal Hedging and Carryover Storage Value. *J. Water Resour. Plan. Manag.* **2004**, *130*, 83–87. https://doi.org/10.1061/(ASCE)0733-9496(2004)130:1(83).
35. You, J.Y.; Cai, X. Hedging rule for reservoir operations: 1. A theoretical analysis. *Water Resour Res.* **2008**, *44*, W01415. https://doi.org/10.1029/2006WR005481.
36. Zeng, X.; Hu, T.; Xiong, L.; Cao, Z.; Xu, C. Derivation of operation rules for reservoirs in parallel with joint water demand. *Water Resour. Res.* **2015**, *51*, 9539–9563. https://doi.org/10.1002/2015WR017250.
37. Allen, R.G.; Pereira, L.S.; Raes, D.; Smith, M. *Crop Evapotranspiration, Guidelines for Computing Crop Water Requirements*; FAO: Rome, Italy, 1998.
38. Fan, Y.; Chen, H.; Gao, Z.; Chang, X. Canal water distribution optimization model based on water supply conditions. *Comput. Electron. Agric.* **2023**, *205*, 10. https://doi.org/10.1016/j.compag.2022.107565.
39. Bayazit, M.; Unal, N.E. Effects of hedging on reservoir performance. *Water Resour. Res.* **1990**, *26*, 713–719. https://doi.org/10.1029/WR026i004p00713.
40. Lund, J.R.; Reed, R.U. Drought water rationing and transferable rations. *J. Water Resour. Plan. Manag.* **1995**, *121*, 429–437. https://doi.org/10.1061/(ASCE)0733-9496(1995)121:6(429).
41. Shiau, J.T. Analytical optimal hedging with explicit incorporation of reservoir release and carryover storage targets. *Water Resour. Res.* 2011, 47, W01515. https://doi.org/10.1029/2010WR009166.
42. Shih, J.S.; Revelle, C. Water-supply operations during drought—Continuous hedging rule. *J. Water Resour. Plan. Manag.* **1994**, *120*, 613–629. https://doi.org/10.1061/(ASCE)0733-9496(1994)120:5(613).
43. Taghian, M.; Rosbjerg, D.; Haghighi, A.; Madsen, H. Optimization of Conventional Rule Curves Coupled with Hedging Rules for Reservoir Operation. *J. Water Resour. Plan. Manag.* **2014**, *140*, 693–698. https://doi.org/10.1061/(ASCE)WR.1943-5452.0000355.
44. Canon, J.; Gonzalez, J.; Valdes, J. Reservoir Operation and Water Allocation to Mitigate Drought Effects in Crops: A Multi-level Optimization Using the Drought Frequency Index. *J. Water Resour. Plan. Manag.* **2009**, *135*, 458–465. https://doi.org/10.1061/(ASCE)0733-9496(2009)135:6(458).
45. Chang, J.; Guo, A.; Wang, Y.; Ha, Y.; Zhang, R.; Xue, L.; Tu, Z. Reservoir Operations to Mitigate Drought Effects with a Hedging Policy Triggered by the Drought Prevention Limiting Water Level. *Water Resour. Res.* **2019**, *55*, 904–922. https://doi.org/10.1029/2017WR022090.
46. Li, Y.; Ding, W.; Chen, X.; Cai, X.; Zhang, C. An Analytical Framework for Reservoir Operation with Combined Natural Inflow and Controlled Inflow. *Water Resour. Res.* **2020**, *56*, 20. https://doi.org/10.1029/2019WR025347.
47. Liu, X.; Guo, S.; Liu, P.; Chen, L.; Li, X. Deriving Optimal Refill Rules for Multi-Purpose Reservoir Operation. *Water Resour. Manag.* **2011**, *25*, 431–448. https://doi.org/10.1007/s11269-010-9707-8.